ORIGINAL ARTICLE
Iran J Allergy Asthma Immunol
August 2026; 25(4):602-616.
DOI: 10.18502/ijaai.v25i4.21746

Regulation of AQP4 Expression and Investigation of the Underlying Mechanisms by HIV-1 Tat Through the NMDAR/cAMP/PKA Signaling Pathway in Astrocytes

Chuo Li[1,2,3], Ran Duan[4], and Congcong Fu[1,2,3]

[1] Department of Neurology, Guangzhou Eighth People's Hospital, Guangzhou Medical University, Guangzhou, China
[2] Institute of Infectious Diseases, Guangzhou Eighth People's Hospital, Guangzhou Medical University, Guangzhou, China
[3] Guangzhou Key Laboratory of Clinical Pathogen Research for Infectious Diseases, Guangzhou, China
[4] The Second Clinical Medical College, Guangzhou University of Chinese Medicine, Guangzhou, China

Received: 6 October 2025; Received in revised form: 19 December 2025; Accepted: 24 December 2025

ABSTRACT

Human immunodeficiency virus (HIV)-associated neurocognitive disorder (HAND) remains a major neurological complication in people living with HIV despite effective antiretroviral therapy. Neurotoxicity caused by viral proteins, particularly the HIV-1 transactivator of transcription (Tat), contributes significantly to HAND. Although N-methyl-D-aspartate receptors (NMDARs) in astrocytes are known to regulate aquaporin-4 (AQP4) the mechanisms by which Tat influences NMDAR signaling and AQP4 expression remain unclear. This study investigated how HIV-1 Tat regulates AQP4 expression in astrocytes through the NMDAR/CaMKII/AC/cAMP/PKA signaling pathway and how secondary Ca^{2+} dynamics modulate this process.

Astrocytic Ca^{2+} influx was measured using the Fluo-3 AM probe. Western blotting quantified *AQP4, NR1, NR2A/B, CaMKII, p-CaMKII, PKA,* and *PKG* expression. Real-time quantitative polymerase chain reaction (RT-qPCR) assessed mRNA levels of AQP4 and NMDAR-related genes. Enzyme-linked immunosorbent assay (ELISA) evaluated nitric oxide synthase activity, adenylate cyclase activity, and intracellular cAMP levels. Pharmacologic inhibitors-MK-801 (NMDAR blocker), H89 (PKA inhibitor), and KT5823 (protein kinase G [PKG] inhibitor)-were applied to investigate pathway interactions.

HIV-1 Tat induced robust activation of NMDAR, resulting in increased Ca^{2+} influx and sequential activation of the CaMKII/AC/cAMP/PKA pathway, ultimately elevating AQP4. After prolonged Tat exposure (approximately 36 hours), a secondary surge in Ca^{2+} activated PKG, which acts as a protective negative feedback mechanism to inhibit excessive NMDAR activity, thereby stabilizing Ca^{2+} influx and preventing abnormal overexpression of *AQP4*. Cotreatment with MK-801, H89, or KT5823 suppressed Tat-induced Ca^{2+} influx and attenuated *AQP4* upregulation, although persistent Tat exposure gradually restored Ca^{2+} elevations through compensatory mechanisms.

Corresponding Author: Chuo Li, MD or PhD;
Department of Neurology, Guangzhou Eighth People's Hospital, Guangzhou Medical University, Guangzhou, China.
Tel: (+860 020) 3647 3857, Fax: (+860 020) 3647 3857, Email: lichuo2030@163.com

HIV-1 Tat dynamically regulates *AQP4* expression in astrocytes via the NMDAR/CaMKII/AC/cAMP/PKA pathway, with PKG-mediated feedback contributing to later stabilization. These findings highlight *AQP4* as a potential therapeutic target for HAND.

Keywords: AQP4; HAND; NMDAR/cAMP/PKA signaling pathway; Tat protein

INTRODUCTION

Upon infection with the human immunodeficiency virus (HIV), individuals may develop acquired immunodeficiency syndrome (AIDS), which is primarily characterized by impaired function of T lymphocytes. The global spread of AIDS has been pervasive for 4 decades, posing a profound threat to human health. According to the report published by the Joint United Nations Program on HIV/AIDS, approximately 1.3 million new cases of HIV infection were reported worldwide in 2022, resulting in a cumulative total of approximately 39 million individuals infected with HIV. Among them, around 29.8 million people received antiretroviral therapy (ART); however, tragically, about 630 000 individuals succumbed to HIV-related diseases. HIV-associated neurocognitive disorder (HAND) stands as one of the most severe complications of HIV infection. It is recognized as a spectrum disorder and is commonly diagnosed through neurocognitive testing, which encompasses the evaluation of attention, memory, executive function, perception, information processing, language, and other domains.[1] With the development and widespread use of ART, although the life expectancy and quality of life of HIV-infected individuals have improved, the incidence of HAND has not decreased significantly like other complications. Previous studies have shown that the incidence of HAND ranges from 21% to 86%[2-4] and increases with age.[5]

HIV does not infect neurons directly, but the neurotoxicity caused by its viral proteins is an important factor in the occurrence of HAND.[6,7] The transactivator of transcription (Tat) is an important regulatory protein encoded by HIV-1, which plays a crucial role in virus replication and also plays an important role in processes such as immune suppression and neuronal damage.[6] In recent years, there have been reports that Tat protein can interact with N-methyl-D-aspartate receptor (NMDAR) in neurons, affecting intracellular Ca^{2+} concentration.[8,9] As a fundamental structure in various physiological and pathological processes in the human central nervous system, NMDAR is not only widely expressed in neurons but also in astrocytes, allowing cells to respond to external signals.[10] NMDARs in astrocytes are heterotetrameric complexes primarily composed of obligatory NR1 subunits and regulatory NR2 (NR2A/B) subunits, which exhibit distinct expression patterns and functional properties. The NR1 subunit is constitutively expressed and forms the core of the receptor channel, essential for Ca^{2+} permeability and receptor trafficking to the cell membrane. In contrast, NR2A and NR2B subunits are dynamically regulated—NR2A is associated with mature synaptic function and mediates rapid, transient Ca^{2+} signaling, while NR2B dominates in immature or reactive astrocytes, contributing to prolonged Ca^{2+} influx and neuroinflammatory responses. While studies have explored Tat's effects on neuronal NMDARs, direct research on the interaction between Tat and astrocytic NMDARs remains scarce, and the underlying regulatory mechanisms remain unclear. Notably, in a model of traumatic brain injury, it has been confirmed that the expression of aquaporin-4 (AQP4) in astrocytic glial cells is regulated by the NMDA signaling pathway.[11] AQP4 is the most abundant water channel protein expressed in the central nervous system. It forms tetramers that traverse the cell membrane and is widely involved in various processes including brain water balance, neuronal excitability, neuroinflammation, neuronal apoptosis, glial scar formation, and neurodegenerative disorders.[12,13] Dysregulation of AQP4 expression plays a significant role in the pathophysiological processes of Alzheimer's disease (AD), which is primarily characterized by cognitive impairment.[14] There is limited research on the relationship between AQP4 and HIV. One study showed that the expression levels of AQP4 in the frontal cortex homogenates of HIV-associated dementia patients were significantly elevated. Immunolabeling of brain tissue indicated patchy AQP4 in reactive astrocytes surrounding blood vessels. This may be related to HIV-induced neuroinflammation, edema, and metabolic disturbances.[15] Research in animal models has found that initially, there is a decrease in AQP4 levels in the

brains of HIV-infected animals, followed by cortical degeneration. It is speculated that AQP4 plays an important role in the development and progression of HAND.[16]

In this study, we hypothesized a priori that HIV-1 Tat protein induces changes in NMDAR and secondary Ca^{2+} influx in astrocytes. We also evaluated the activation of the calcium/calmodulin-dependent protein kinase II (CaMKII)/adenylate cyclase (AC)/cyclic adenosine monophosphate (cAMP)/protein kinase A (PKA) signaling pathway and the protein kinase G (PKG) signaling pathway after the change in Ca^{2+} concentration, and investigated the effect of HIV-1 Tat on AQP4 expression in astrocytes. Unlike previous studies that primarily focused on Tat-induced neuronal damage or isolated roles of NMDAR or AQP4 in HAND, our work innovatively dissects the temporal dynamic regulatory network linking HIV-1 Tat to AQP4 expression—specifically highlighting the sequential activation of NMDAR/CaMKII/AC/cAMP/PKA and the subsequent PKG-mediated feedback inhibition. By integrating pharmacologic inhibition (MK-801, H89, KT5823) with multidimensional assays, we provide the first direct evidence that Tat modulates AQP4 through this cascade in astrocytes, filling the critical gap in understanding how astrocytic NMDAR signaling contributes to HAND pathogenesis. The results showed that HIV-1 Tat regulates AQP4 expression in astrocytes through the NMDAR/cAMP/PKA signaling pathway, which is involved in the pathological and physiological processes of HAND. This study not only identifies AQP4 as a novel therapeutic target for HAND but also offers a mechanistic framework for developing pathway-specific interventions, addressing the unmet clinical need for effective treatments against HAND despite ART advancements.

MATERIALS AND METHODS

Isolation and Culture of Astrocytes

The bilateral cerebral cortex tissues from 1-day-old Sprague-Dawley (SD) rats (provided by Beijing Vital River Laboratory Animal Technology Co, Ltd, Beijing, China) were isolated. The tissues were gently triturated and dispersed in D-Hanks solution. After a period of sedimentation, the supernatant was collected and filtered, followed by centrifugation at 1500 rpm for 5 minutes. The cells were then suspended in DMEM Medium (Hyclone, South Logan, UT, USA) containing 10% newborn calf serum (Gibco, Rockville, MD, USA) and evenly seeded into PLL-coated culture flasks (Falcon, China). All animal experiments were conducted in accordance with the Guide for the Care and Use of Laboratory Animals (NIH, 8th edition, 2011). The culture flasks were placed in a 37 °C incubator with 5% CO_2 for static cultivation. Every 3 days, one-third of the culture medium was replaced. On the 9th day, the culture medium was discarded, and the cells were rinsed twice with prewarmed D-Hanks solution. Subsequently, 0.25% trypsin-EDTA digestion solution was added and incubated at 37 °C for 3 to 5 minutes (digestion was terminated when cell adherence was loosened and intercellular gaps were enlarged). The digestion was stopped by adding an equal volume of complete medium (DMEM + 10% newborn calf serum), and the cell suspension was gently pipetted to form a single-cell suspension for subculturing.

Identification of Astrocytes

The cultured astrocytes at the P3 generation were fixed with 4% paraformaldehyde for 15 minutes. Subsequently, they were washed 3 times with PBS (Hyclone, South Logan, UT, USA) for 3 minutes each, followed by permeabilization with 0.5% Triton X-100 at room temperature for 20 minutes. After another 3 washes with PBS for 3 minutes each, the liquid was removed, and the samples were blocked with goat serum at room temperature for 30 minutes. The blocking solution was removed, and the samples were incubated overnight at 4 °C with anti-GFAP antibody (Abcam, ab7260, Cambridge, MA, USA). Then, the samples were washed 3 times with PBST (PBS with 0.1% Tween-20) for 3 minutes each, the liquid was removed, and Goat Anti-Rabbit IgG H&L (FITC, 1:500) (Abcam, ab6717, Cambridge, MA, USA) was added and incubated for 1 hour. After another 3 washes with PBST for 3 minutes each, DAPI was added and incubated for 5 minutes in the dark. Finally, the samples were washed 4 times with PBST for 5 minutes each, the liquid was removed, 50% glycerol was added, and the samples were observed and imaged using a fluorescence microscope (Olympus, Tokyo, Japan).

The Primary Astrocytes Were Divided into Distinct Groups for Cultivation

The primary astrocytes were divided into 5 groups for culture: the Control group, the HIV-1 Tat group, the HIV-1 Tat+MK-801 group, the HIV-1 Tat+H89 group,

and the HIV-1 Tat+KT5823 group. The Control group did not receive any drug treatment. The HIV-1 Tat group was pretreated with 1 μg/mL of HIV-1 Tat 18 (Abcam, ab83353, Cambridge, MA, USA). The HIV-1 Tat+MK-801 group was pretreated with 1 μg/mL of HIV-1 Tat and 5 μg/mL of MK-801 (MedChemExpress, HY-15084B, Monmouth Junction, NJ, USA). The HIV-1 Tat+H89 group was pretreated with 1 μg/mL of HIV-1 Tat and 5 μg/mL of H89 (MedChemExpress, HY-15979, Monmouth Junction, NJ, USA). The HIV-1 Tat+KT5823 group was pretreated with 1 μg/mL of HIV-1 Tat and 5 μg/mL of KT5823 (MedChemExpress, HY-N6791, Monmouth Junction, NJ, USA). After a 30-minute incubation, all groups were exposed to 10 μmol/L of NMDA (MedChemExpress, HY-17551, Monmouth Junction, NJ, USA). Various assays were performed at 1, 2, 4, 8, 12, 16, 20, 24, 36, 48, and 72 hours following the addition of NMDA.

Measurement of Intracellular Ca^{2+} Concentration

The astrocytes from different groups were harvested, and the intracellular Ca^{2+} concentration was determined using Fluo-3 AM, a fluorescent calcium ion probe (Solarbio, Beijing, China). Firstly, the cells were washed 3 times with HBSS solution. Subsequently, they were incubated with the Fluo-3 AM working solution at 37 °C in a cell culture incubator for 30 minutes. Next, the cells were washed 3 times with HEPES-buffered saline solution and then incubated with HBSS solution containing 1% fetal bovine serum at 37 °C in a cell culture incubator for an additional 30 minutes. The cells were then resuspended in HEPES-buffered saline solution and adjusted to a concentration of 1×10^5 cells/mL. The intracellular Ca^{2+} concentration was measured using a fluorescence microplate reader. Data analysis was conducted using the formula $[Ca^{2+}]=K_d\times[(F-F_{min}) / (F_{max} -F)\times(E/T)]$ (nmol/L). F_{min} (minimum fluorescence intensity) was determined by adding 2 mmol/L EGTA to chelate free Ca^{2+}; F_{max} (maximum fluorescence intensity) was measured after adding 5 mmol/L $CaCl_2$ to saturate the Fluo-3 AM probe. The dissociation constant (Kd) of 345 nmol/L was used as specified by the Fluo-3 AM manufacturer (Solarbio, Beijing, China).

Real-time PCR Detection

Astrocytes from different groups were collected, and RNA extraction from the samples was performed using TRNzol (TIANGEN, Beijing, China). The concentration and purity of the extracted RNA were determined using a spectrophotometer (Thermo Scientific, Waltham, MA, USA). Subsequently, cDNA reverse transcription was carried out using the PrimeScript RT reagent Kit with gDNA Eraser (TaKaRa, Tokyo, Japan), following the experimental procedures outlined in the product manual. All cDNA samples were then prepared and configured for the real-time PCR reaction system (TaKaRa, Tokyo, Japan), and PCR reactions were conducted on a real-time PCR instrument (Thermo Scientific, Waltham, MA, USA). Data analysis was performed using the $2^{-\Delta\Delta CT}$ method. The primer sequences for the target genes are presented in Supplementary Table S1.

Western Blotting Detection

Astrocytes from different groups were collected, and total protein was extracted using a RIPA lysis buffer supplemented with 1% phenylmethylsulfonyl fluoride (PMSF) and 1% protease/phosphatase inhibitor cocktail (Thermo Scientific, USA) to prevent protein degradation and dephosphorylation. The protein concentration was determined via the Bicinchoninic Acid (BCA) Protein Assay Kit (Thermo Scientific, USA) following the manufacturer's instructions. Each sample (30 μg) was loaded onto a 10% SDS-PAGE gel for electrophoretic separation at 80 V for 30 minutes (stacking gel) and 120 V for 90 minutes (resolving gel), and subsequently transferred to a PVDF membrane (Millipore, USA) via wet transfer at 200 mA for 90 minutes. The PVDF membrane was then blocked with a TBST solution (10 mM Tris-HCl, 150 mM NaCl, 0.1% Tween-20, pH 7.4) containing 5% skim milk at room temperature for 1 hour. Subsequently, according to previous protocols[17,18], the membrane was incubated overnight at 4 °C with primary antibodies (diluted 1:1000 in TBST containing 5% skim milk), including anti-AQP4 (Affinity Biosciences, AF5164), anti-NR1 (Affinity Biosciences, AF6406), anti-NR2A (Affinity Biosciences, DF7955), anti-NR2B (Affinity Biosciences, AF6426), anti-CaMKII (Affinity Biosciences, DF2907), anti-p-CaMKII (Affinity Biosciences, AF7378), anti-PKA (Affinity Biosciences, AF7746), anti-PKG (Epigentek, A-7418), and anti-GAPDH (Affinity Biosciences, AF7021; used as an internal reference, diluted 1:5000). Following this, the membrane was washed 3 times with TBST (5 minutes per wash), and the corresponding secondary antibodies, including Goat Anti-Rabbit IgG H&L (HRP) (Abcam, ab205718; diluted 1:5000) and Goat Anti-Mouse IgG H&L (Abcam, ab175783; diluted

1:5000), were added and incubated for 45 minutes at room temperature. After incubation, the membrane was washed 3 times with TBST (5 minutes per wash) again. Finally, the PVDF membrane was incubated with an ECL chemiluminescence working solution (Thermo Scientific, USA) at room temperature for 5 minutes in the dark. The membrane was scanned using a ChemiDoc XRS+ Imaging System (Bio-Rad, USA) to obtain an electronic image, and Quantity-One image analysis software (Bio-Rad, USA) was employed for data analysis by calculating the gray value ratio of target protein bands to GAPDH bands to normalize protein expression levels.

ELISA Detection

Astrocytes were collected from different experimental groups and diluted in PBS to a cell density of 1×10^9 cells/L. The cell suspensions were subjected to sonication using an ultrasonic cell disruptor for 5 cycles of 30 seconds each. Following sonication, the disrupted cells were centrifuged at 2000 rpm for 20 minutes at 4 °C, and the resultant supernatants were collected. Adenylate cyclase activity levels were determined using an Adenylate Cyclase Assay Kit (Nanjing Jiancheng Bioengineering Institute, Nanjing, China). The levels of cAMP were quantified using a cyclic AMP ELISA Kit (Solarbio, Beijing, China), and the activity of nitric oxide synthase (NOS) was assessed using a Nitric Oxide Synthase Assay Kit (Nanjing Jiancheng Bioengineering Institute, Nanjing, China). All experimental procedures were performed in accordance with the instructions provided with the assay kits. The adenylate cyclase activity levels, cAMP levels, and NOS activity levels were calculated using the formulas provided in the assay kit instructions.

Statistical Analysis

The data were analyzed and plotted using GraphPad Prism 5.0 (La Jolla, CA, USA). The results of the experiments were expressed as the mean and standard deviation (mean ± SD) through 3 repeated experiments.

RESULTS

The Morphology and Identification of Astrocytes

Under in vitro culture conditions, astrocytes were observed to exhibit a ramified morphology with multiple dendritic processes, forming a star-shaped structure. The nuclei of the cells appeared relatively large and exhibited predominantly circular or elliptical shapes (Figure 1A). Immunofluorescent staining of astrocytes using glial fibrillary acidic protein (GFAP) revealed the presence of GFAP-positive cells, which exhibited green fluorescence, while the cell nuclei displayed blue fluorescence (Figure 1B).

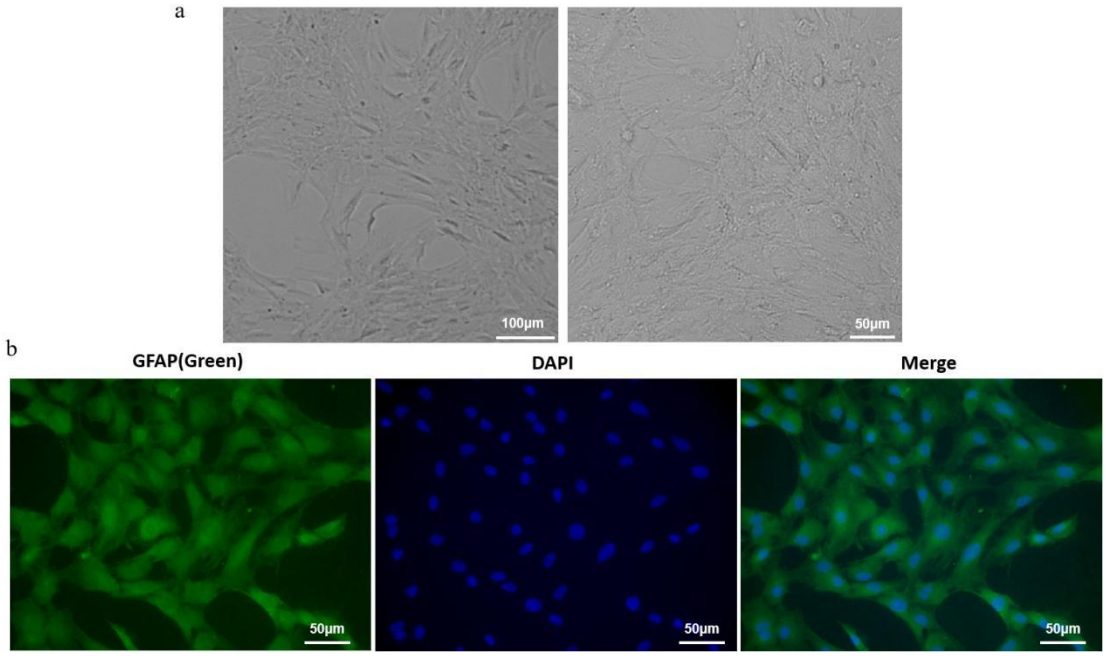

Figure 1. (A) Morphology of astrocytes. (B) Immunofluorescent identification of astrocytes.

Published by Tehran University of Medical Sciences (http://ijaai.tums.ac.ir)

HIV-1 Tat Triggers Time-Dependent Calcium Influx via NMDAR and Its Downstream Kinases

In order to determine the intracellular Ca^{2+} concentration, the glial cells were cultured and divided into different groups (Figure 2). To ensure the reliability of Ca^{2+} detection, we verified the linearity of the Ca^{2+} signal using Ca^{2+} standard solutions to avoid potential saturation of the FURA calcium sensor; no sensor saturation was observed throughout the experiment. During the entire culture period (1-72 hours), the intracellular Ca^{2+} in the control group remained at a low level without significant fluctuation. In the HIV-1 Tat group, Ca^{2+} concentration increased significantly (p<0.05) from 8 hours after NMDA treatment and maintained a persistently high level at multiple time points, including 12, 16, 20, 24, 36, 48, and 72 hours. To further clarify the regulatory mechanism, we introduced the NMDAR antagonist MK-801, the PKA inhibitor H89, and the PKG inhibitor KT5823. The results showed that Ca^{2+} levels in the HIV-1 Tat+MK-801 group, HIV-1 Tat+H89 group, and HIV-1 Tat+KT5823 group were all significantly lower than those in the HIV-1 Tat group (p<0.001), suggesting that MK-801 can inhibit Tat-induced calcium elevation by blocking NMDA receptors, and both the PKA pathway (intervened by H89) and PKG pathway (intervened by KT5823) are involved in the regulation of this calcium signaling process. In conclusion, HIV-1 Tat can significantly enhance NMDA-induced intracellular calcium signaling, and this effect depends on the activation of NMDA receptors and involves the participation of PKA and PKG signaling pathways.

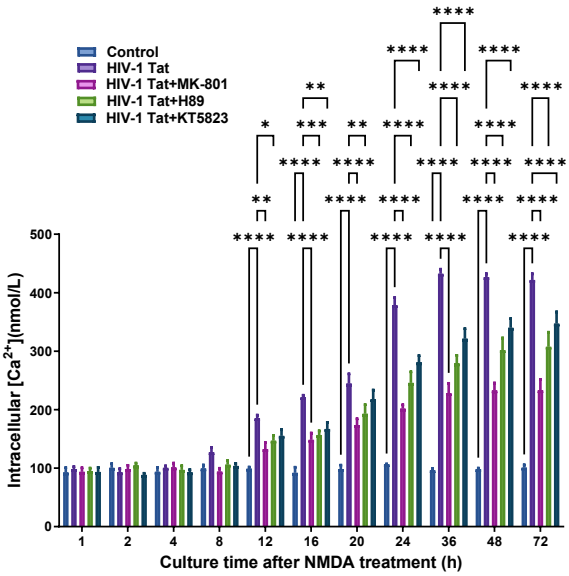

Figure 2. Intracellular Ca^{2+} concentration was measured at 1, 2, 4, 8, 12, 16, 20, 24, 36, 48, and 72 hours after the addition of NMDA in astrocytes cultured in different groups.

NMDAR Pathway Activation Drives the Transcriptional Upregulation of AQP4 and NMDAR Subunits

Subsequently, the mRNA expression levels of *AQP4*, NMDAR subunits (*NR1*, *NR2A*, *NR2B*), and *CaMKII* in astrocytes were detected to explore the regulatory effects of HIV-1 Tat and related inhibitors (Figure 3). The results showed that, compared with the control group, the mRNA expression levels of *AQP4*, *NR2A*, and *CaMKII* in the HIV-1 Tat group increased continuously from 1 to 72 hours, peaking at 72 hours, while the mRNA expression levels of *NR1* and *NR2B* also increased continuously, peaking at 48 hours. In the HIV-1 Tat+MK-801 group, HIV-1 Tat+H89 group, and HIV-1 Tat+KT5823 group, the mRNA expression levels of each molecule were lower than those in the HIV-1 Tat group during the corresponding time periods (e.g., 8-72 hours for *AQP4*, 4-72 hours for *NR1*, etc.), but they still showed an upward trend and stabilized or peaked at specific time points (e.g., 24, 36, 48 hours, etc.). In conclusion, HIV-1 Tat can significantly upregulate the mRNA expression of *AQP4*, NMDAR subunits (*NR1*,

NR2A, *NR2B*), and *CaMKII*, and this process involves the participation of NMDA receptors and the PKA and PKG signaling pathways.

Protein-level Confirmation of Signaling Pathway Activation and Kinase Crosstalk

We next confirmed these findings at the protein level. Western blot analysis mirrored the transcriptional data, showing that HIV-1 Tat significantly increased the protein abundance of AQP4, NR1, NR2A, NR2B, PKA, and PKG (Figure 4). Compared to the Control group, the HIV-1 Tat group exhibited an increasing trend in the protein expression levels of AQP4, NR2A, NR2B, PKA, and PKG from 12 to 72 hours, with the peak observed at 72 hours (Figure 4A, 4C, 4D, 4F, and 4G). Similarly, the protein expression levels of NR1 showed a progressive increase from 2 to 72 hours, reaching the highest point at 72 hours (Figure 4B). The ratio of p-CaMKII/CaMKII displayed an ascending trend from 12 to 72 hours, reaching its peak at 48 hours and subsequently stabilizing (Figure 4E). Compared to the HIV-1 Tat group, the protein expression levels of AQP4, NR2A, NR2B, PKA, and PKG in the HIV-1 Tat+MK-801, HIV-1 Tat+H89, and HIV-1 Tat+KT5823 groups were relatively lower from 12 to 72 hours, yet they exhibited a consistent upward trend, reaching their peak at 72 hours (Figure 4A, 4C, 4D, 4F, and 4G). Similarly, the protein expression levels of NR1 were relatively lower from 2 to 72 hours, but displayed a progressive increase, peaking at 72 hours (Figure 4B). Likewise, the ratio of p-CaMKII/CaMKII was relatively lower from 12 to 72 hours, but demonstrated an ascending trend, reaching its highest peak at 72 hours (Figure 4E).

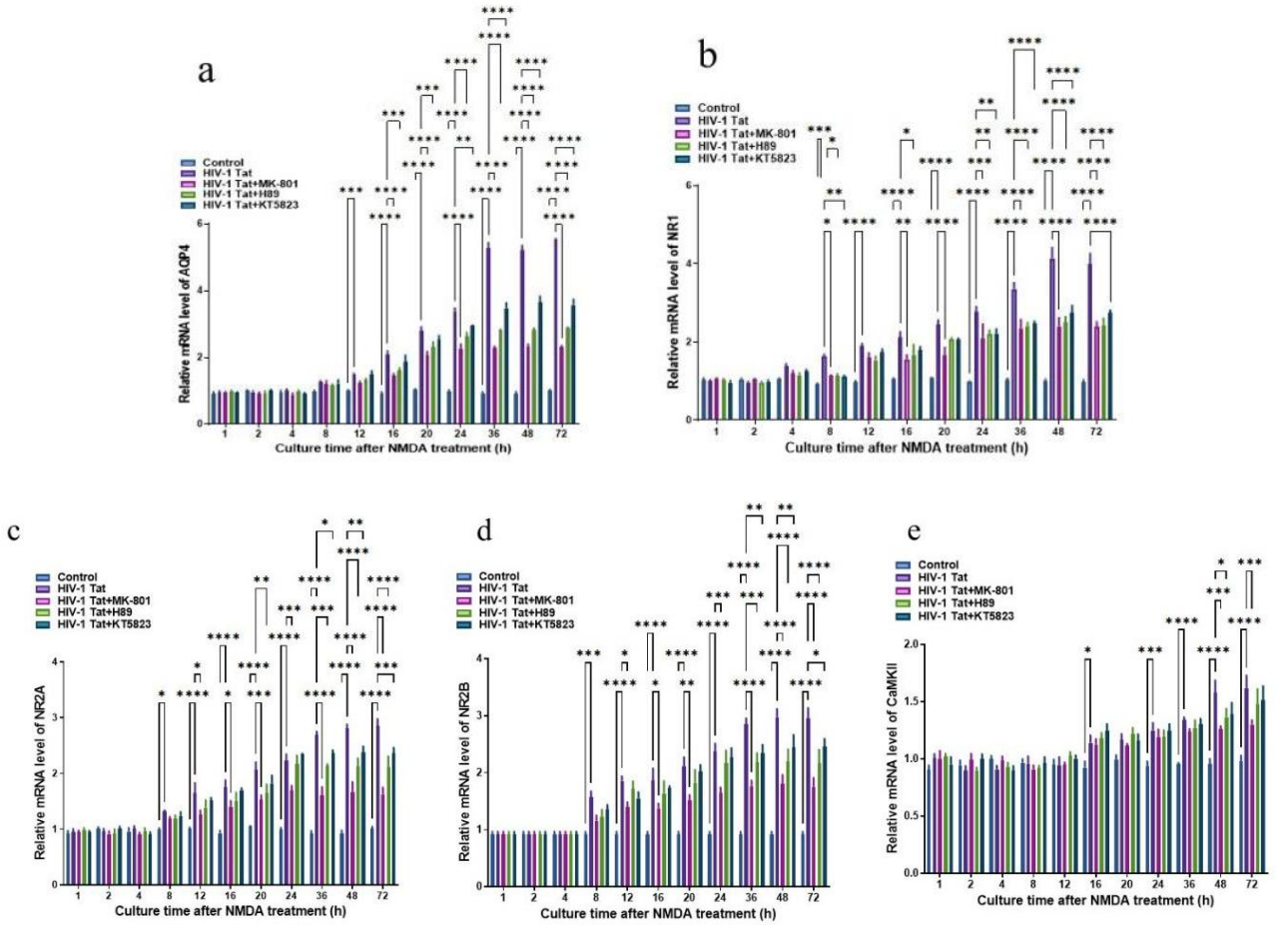

Figure 3. In astrocytes cultured in separate groups, the mRNA expression levels of target genes were determined using real-time fluorescence quantitative PCR at 1, 2, 4, 8, 12, 16, 20, 24, 36, 48, and 72 hours after NMDA administration. (A) mRNA expression levels of *AQP4*. (B) mRNA expression levels of *NR1*. (C) mRNA expression levels of *NR2A*. (D) mRNA expression levels of *NR2B*. (E) mRNA expression levels of *CaMKII*.

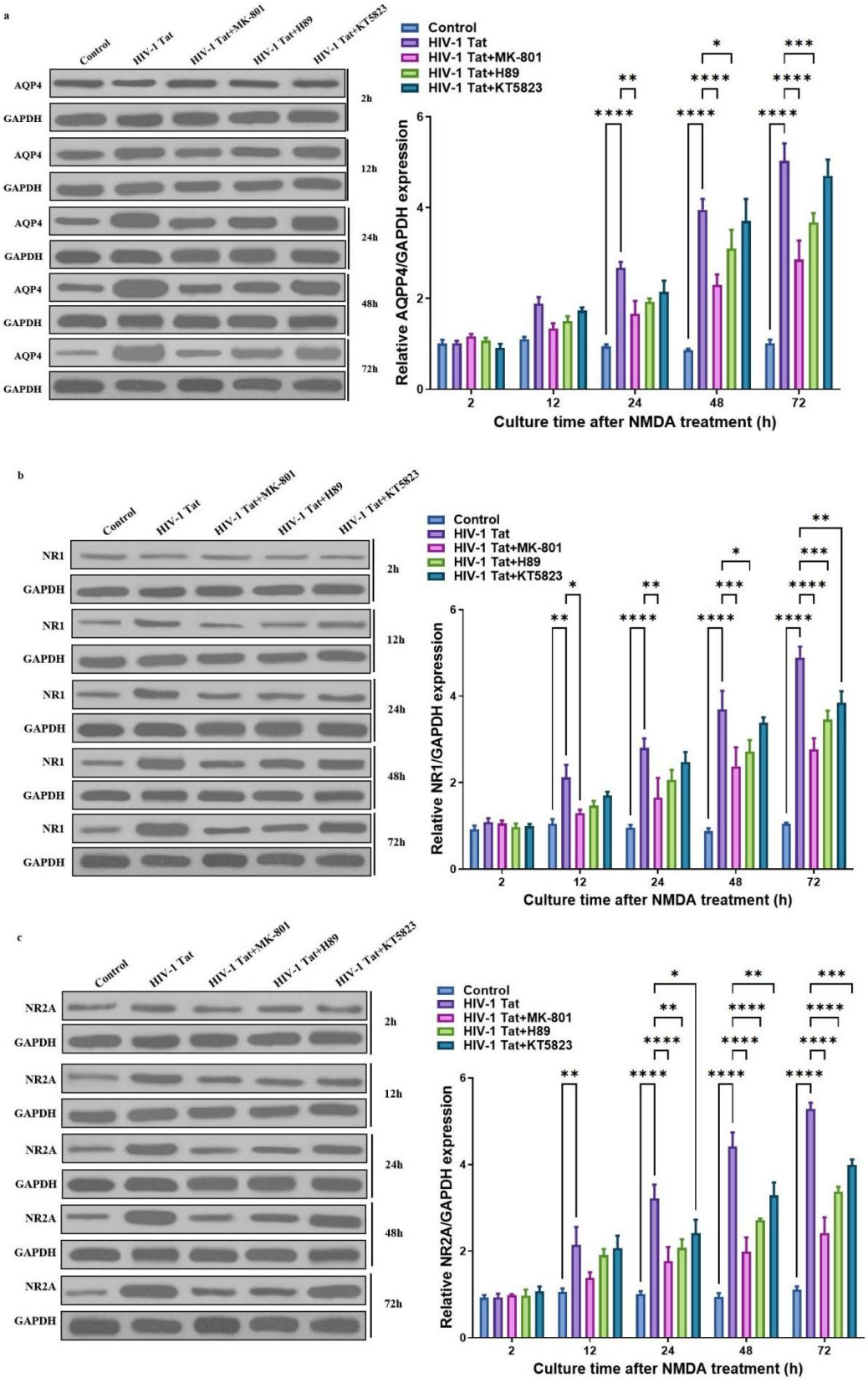
a
Control
HIV-1 Tat
HIV-1 Tat+MK-801
HIV-1 Tat+H89
HIV-1 Tat+KT5823
AQP4
GAPDH
2h
12h
24h
48h
72h
Relative AQPP4/GAPDH expression
Culture time after NMDA treatment (h)
b
NR1
Relative NR1/GAPDH expression
c
NR2A
Relative NR2A/GAPDH expression

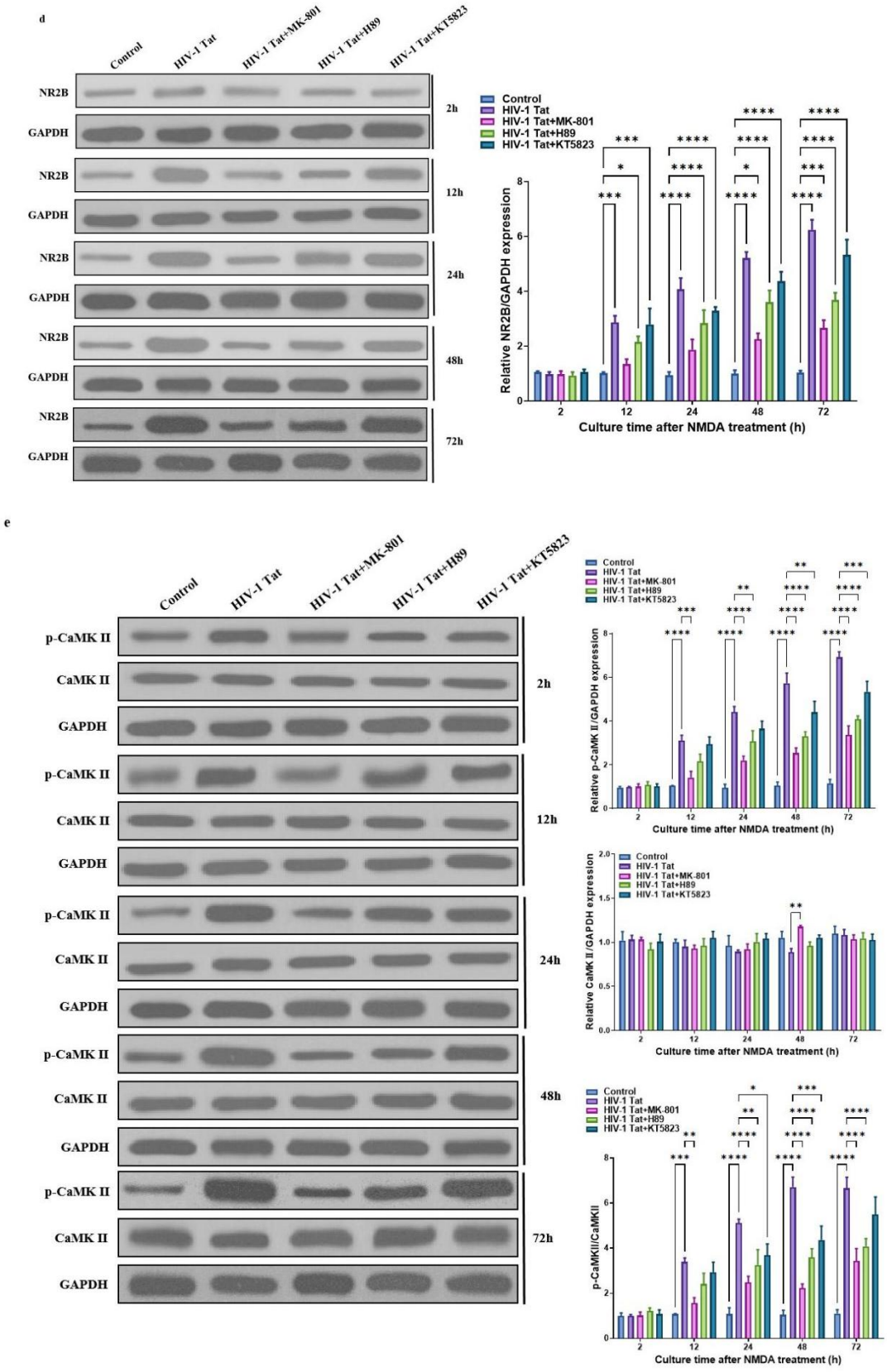

Published by Tehran University of Medical Sciences (http://ijaai.tums.ac.ir)

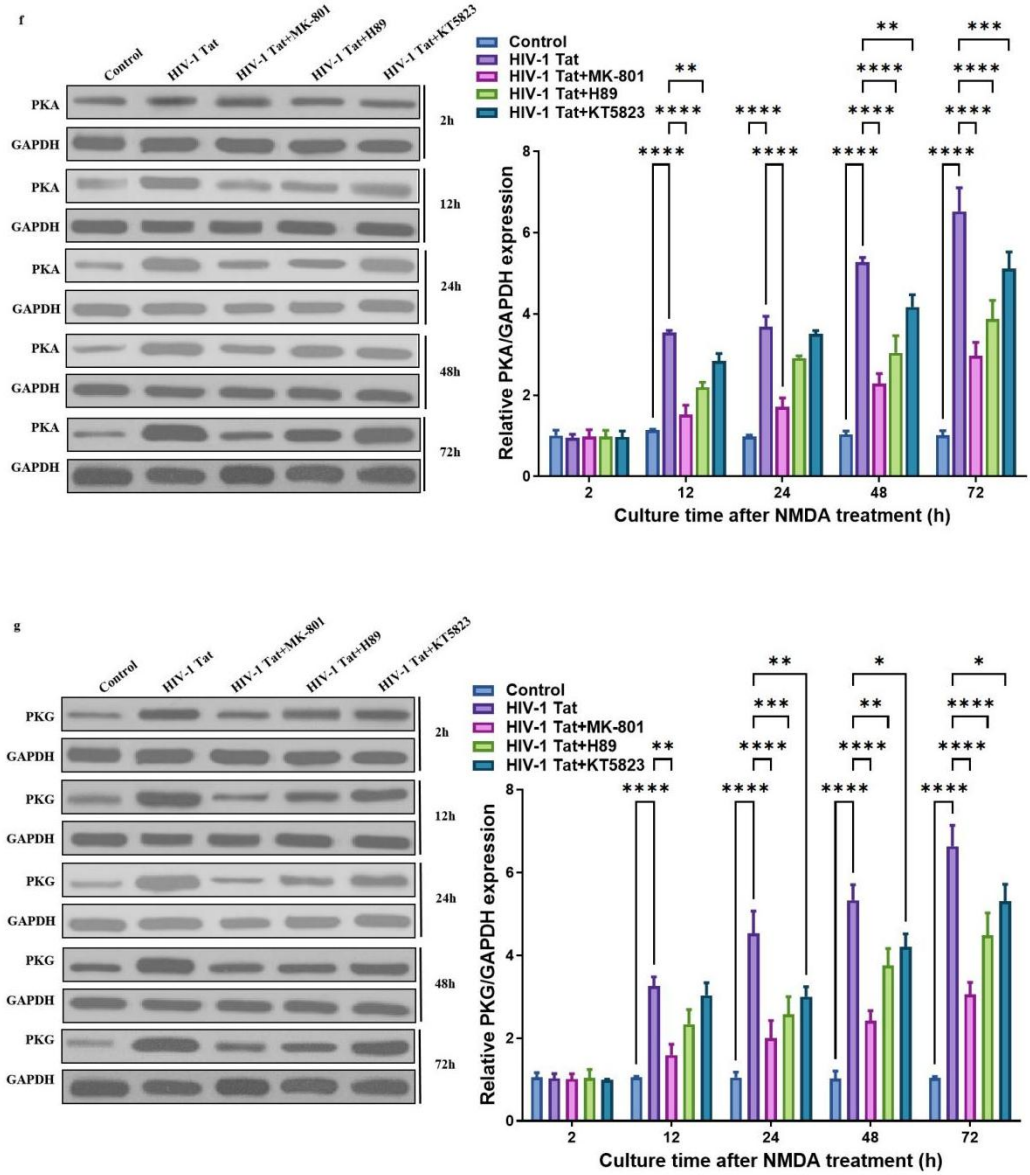

Figure 4. In astrocytes cultured in separate groups, the protein expression levels of target proteins were assessed using Western blot analysis at 2, 12, 24, 48, and 72 hours post NMDA administration. (A) Protein expression levels of AQP4. (B) Protein expression levels of NR1. (C) Protein expression levels of NR2A. (D) Protein expression levels of NR2B. (E) Protein expression levels of p-CaMKII and CaMKII. (F) Protein expression levels of PKA. (G) Protein expression levels of PKG.

HIV-1 Tat Differentially Regulates Adenylate Cyclase Activity, cAMP and NOS Activities Downstream of NMDAR

The study further detected the activity of adenylate cyclase (AC), the level of cyclic adenosine monophosphate (cAMP), and the activity of nitric oxide synthase (NOS) in astrocytes to explore the regulatory effects of HIV-1 Tat and related inhibitors (Figure 5). The results showed that, compared with the control group, the AC activity in the HIV-1 Tat group showed an upward trend from 1 to 72 hours, peaking at 20 hours followed by a slight decline; the cAMP level increased continuously from 4 to 72 hours, peaking at 72 hours; and the NOS activity exhibited a downward trend from 1 to 72 hours, reaching the lowest level at 72 hours. In the HIV-1 Tat+MK-801 group, HIV-1 Tat+H89 group, and HIV-1 Tat+KT5823 group, the AC activity was lower than that in the HIV-1 Tat group from 1 to 72

hours but still showed an upward trend, stabilizing or changing at specific time points (after 20, 36, or 16 hours); the cAMP level was lower than that in the HIV-1 Tat group from 4 to 72 hours but still maintained an upward trend, with all peaking at 72 hours; and the NOS activity was higher than that in the HIV-1 Tat group during the corresponding time periods (4-72 hours or 8-72 hours) but still showed a downward trend, stabilizing at specific time points (after 48, 72, or 48 hours). In conclusion, HIV-1 Tat can regulate AC activity, cAMP level, and NOS activity in astrocytes, and this process involves the participation of NMDA receptors as well as the PKA and PKG signaling pathways, while the AC/cAMP pathway and NOS may play a role in this process.

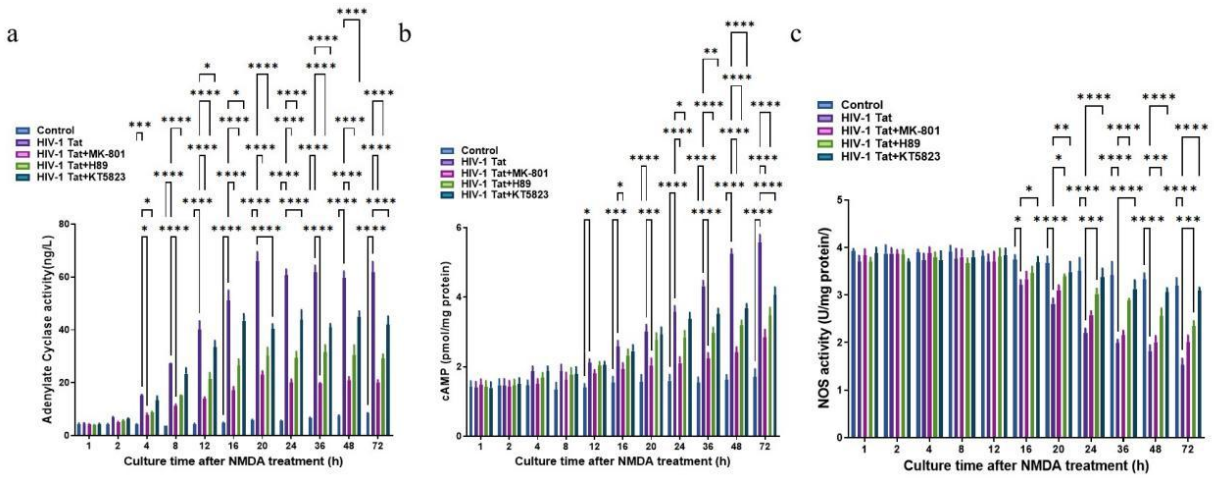

Figure 5. The levels of intracellular adenylate cyclase activity, cAMP, and NOS activity were measured at 1, 2, 4, 8, 12, 16, 20, 24, 36, 48, and 72 hours after the addition of NMDA in astrocytes cultured in different groups.

DISCUSSION

With the development and widespread use of antiretroviral therapy, HIV-infected individuals typically have a life expectancy close to normal.[19] However, age-related complications are also increasing gradually, and HAND is one of the most severe complications. A meta-analysis summarized that the prevalence of HAND in adult HIV patients in the global ART era is 42.6%,[20] and the average time from diagnosis to death for patients is approximately 4 to 6 months. The revised Frascati diagnostic criteria from 2007 are currently the most widely used diagnostic criteria for HAND. These criteria classify HAND into asymptomatic neurocognitive impairment (ANI), mild neurocognitive disorder (MND), and HIV-associated dementia (HAD) based on the severity of cognitive impairment.[21] HAND is not only a challenging medical issue but also increasingly becoming a significant social problem.[22]

The mechanisms of HAND are still under investigation, but viral proteins or neurotoxic extracellular environments are important contributing factors to HAND. In the brain, HIV infects macrophages and microglial cells but does not infect neurons. Therefore, HIV-induced neurotoxicity acts indirectly and is the result of the release of neurotoxic substances such as inflammatory factors, nitric oxide, glutamate, and viral proteins.[23] The transactivator of transcription is a protein released by HIV-1 infected cells. It not only plays a role in the viral transactivation process but also may be involved in the development of HAND. In recent years, several researchers have reported that Tat can activate the FOXO3 factor, leading to neuronal apoptosis.[24] Additionally, Tat can induce neuronal autophagy by upregulating Bcl-2-associated athanogene 3 (BAG3) through the NF-κB signaling pathway.[25] Upregulation of histone deacetylase expression in neuronal cells inhibits dendritic plasticity.[26] Furthermore, lipid peroxidation and metabolic disturbances contribute to neuronal dysfunction.[27,28] There is limited research on Tat-induced damage to astrocytes and its contribution to HAND. Some researchers have suggested that Tat mediates miR-34a and miR-138, which downregulate SIRT1 and promote astrocyte activation.[29] Tat exhibits significant antioxidant effects and promotes the survival of

astrocytes by resisting cell damage. However, when transported along neural pathways to distant sites, Tat can cause neuronal damage.[30] Research has found that HIV-infected individuals without HAND have higher levels of anti-Tat antibodies in their cerebrospinal fluid compared to those with HAND. This suggests that the antibody response to Tat may have a neuroprotective effect.[31] Despite the significant improvement in the efficacy of HIV infection treatment with antiretroviral therapy, current treatment regimens have not been able to completely halt the production and release of Tat.[32] Therefore, targeting the toxic effects of Tat protein on neuronal cells may be a suitable therapeutic target.

NMDARs are a type of glutamate-gated, calcium-permeable neurotransmitter receptors that primarily control synaptic plasticity and initiate adaptive transcriptional responses for memory formation and learning-related neuroprotection. NR1 is the essential functional subunit of NMDAR, containing the binding site for Ca^{2+} channels, while NR2 is the regulatory subunit containing the NMDA binding site. In in vitro models, neuronal exposure to HIV-1 Tat has shown key aspects of NMDAR involvement in the mechanisms of HAND. HIV-1 Tat enters cells via low-density lipoprotein receptor-related protein-1 (LRP) and within 12 hours activates NMDAR through the tyrosine kinase (SRC) pathway. After 12 hours of Tat exposure, secondary enhanced Ca^{2+} influx inhibits NMDAR through the NOS/SGC/PKG pathway, reducing Ca^{2+} influx.[8,9] Initially, HIV-1 Tat enhances NMDAR activity, but subsequently, NMDAR adapts to the presence of Tat. This adaptive response prevents excessive activation of NMDAR, but it can also lead to excitatory synapse loss associated with HAND.[33] Prolonged exposure of astrocytes to NMDA leads to a significant decrease in AQP4 expression. However, in cells lacking Ca^{2+} or in cells where NMDAR is silenced using corresponding siRNA, no changes in AQP4 were observed.[34] This suggests that NMDAR in astrocytes and its mediated Ca^{2+} influx may play an important role in regulating AQP4. AQP4 is the most abundant water channel protein in the brain and is widely expressed on the cell membranes of astrocytes, with the highest expression in their endfeet, resulting in a polarized distribution.[35-37] This highly polarized AQP4 is not only an important component of the blood-brain barrier but also a major functional structure of the glymphatic system. Its expression plays a crucial role in maintaining the integrity of the blood-brain barrier and normal glymphatic system function.[37-39] Therefore, changes in AQP4 levels may lead to imbalance in water homeostasis, disruption of the blood-brain barrier, and accumulation of metabolic waste products.[40,41] A study using SIVmac239, SIVsm543-3, and SHIV monkey models evaluated changes in AQP4 levels and distribution in the frontal cortex. In the brains of non-infected control animals, AQP4 was uniformly expressed in the subpial and perivascular regions of the cortex. However, in the brains of infected animals, AQP4 labeling was mainly restricted to astrocyte-like cells and lost its uniform distribution. The areas devoid of AQP4 labeling exhibited dense intracellular glial fibers.[17] These findings support the notion that viral infection does indeed alter the expression and distribution of AQP4 in the brain. Some researchers have reported that the cAMP/PKA signaling pathway contributes to AQP4 expression.[42,43] Ca^{2+}/CaMKII is a downstream signaling molecule of NMDAR.[44] It can activate adenylate cyclase to catalyze the conversion of adenosine triphosphate to cyclic adenosine monophosphate, thereby upregulating the expression of AQP4 through the cAMP/PKA signaling pathway.[45-47] On the other hand, in the late stage of Tat exposure, elevated intracellular Ca^{2+} activates PKG as a protective negative feedback mechanism, which specifically inhibits excessive NMDAR activation to reduce Ca^{2+} overload, ultimately stabilizing AQP4 expression and preventing astrocyte dysfunction.[8,9] Consequently, this may lead to the downregulation of AQP4 expression.

In this study, we induced the expression of AQP4 in astrocytes using HIV-1 Tat protein, which initially activated NMDAR and enhanced Ca^{2+} influx, leading to the activation of the CaMKII/AC/cAMP/PKA pathway. However, after 36 hours of induction, the secondary Ca^{2+} surge activates PKG-a protective negative feedback mediator-that inhibits excessive NMDAR activity, thereby attenuating Ca^{2+} influx and stabilizing cellular homeostasis. This led to a stabilization of the expression of NMDAR/CaMKII/AC/cAMP/PKA pathway-related factors and AQP4. Concurrently, we administered the NMDAR antagonist MK-801, PKA inhibitor H89, and PKG inhibitor KT5823 during HIV-1 Tat protein induction. The results showed that HIV-1 Tat regulates the expression of AQP4 in astrocytes through the NMDAR/cAMP/PKA signaling pathway, which is involved in the pathophysiology of HIV-associated

neurocognitive disorders. This provides a novel target, AQP4, for the treatment of HAND.

Although our study provides evidence for a novel mechanism by which HIV-1 Tat regulates AQP4 in astrocytes via the NMDAR/cAMP/PKA pathway, several limitations should be acknowledged. Firstly, the lack of key 'TAT-only' and inhibitor treatment groups limits our ability to precisely define the independent effects of Tat and to rule out potential off-target effects of inhibitors. Secondly, we relied primarily on pharmacological approaches and failed to use genetic tools such as NMDAR siRNA to further validate receptor specificity. Furthermore, the exact origin of the persistent calcium signal observed under MK-801 blockade, such as other ion channels or intracellular calcium stores, remains to be elucidated in future studies. Finally, all conclusions are based on in vitro cell experiments, and their in vivo pathophysiological significance needs to be further validated in animal models.

The results of this study demonstrate that HIV-1 Tat protein can regulate AQP4 expression through the NMDAR/cAMP/PKA signaling pathway, thereby participating in the pathological and physiological processes of HAND. This provides a new target, AQP4, for the treatment of HAND, and lays a theoretical foundation for the targeted development of more effective drugs for HAND. The ultimate goal is to alleviate the burden of the disease and achieve significant societal benefits.

STATEMENT OF ETHICS

These experiments were approved by the Animal Care and Utilization Committee of Guangzhou Medical University Animal Center (IACUC-gz8h-FCC-2023-1) and the protocols complied with the guidelines for the welfare and use of animals.

FUNDING

This work was supported by the Guangzhou Science and Technology plan project (2023A03J0628) and Medical Scientific Research Foundation of Guangdong Province (A2022491).

CONFLICT OF INTEREST

The authors declare no conflicts of interest.

ACKNOWLEDGMENTS

Not applicable.

DATA AVAILABILITY

The data that support the findings of this study are available from the corresponding author upon reasonable request.

AI ASSISTANCE DISCLOSURE

ChatGPT was used in language improvement of this manuscript.

REFERENCES

1. Spooner R, Ranasinghe S, Urasa S, Yoseph M, Koipapi S, Mukaetova-Ladinska EB, et al. HIV-Associated Neurocognitive Disorders: The First Longitudinal Follow-Up of a cART-Treated Cohort of Older People in Sub-Saharan Africa. Jaids-J Acq Imm Def. 2022;90(2):214-22.
2. Wei J, Hou J, Su B, Jiang T, Guo C, Wang W, et al. The Prevalence of Frascati-Criteria-Based HIV-Associated Neurocognitive Disorder (HAND) in HIV-Infected Adults: A Systematic Review and Meta-Analysis. Front Neurol. 2020;11:581346.
3. McDonnell J, Haddow L, Daskalopoulou M, Lampe F, Speakman A, Gilson R, et al. Minimal cognitive impairment in UK HIV-positive men who have sex with men: effect of case definitions and comparison with the general population and HIV-negative men. Jaids-J Acq Imm Def. 2014;67(2):120-7.
4. Rosenthal LS, Skolasky RL, Moxley RTT, Roosa HV, Selnes OA, Eschman A, et al. A novel computerized functional assessment for human immunodeficiency virus-associated neurocognitive disorder. J Neurovirol. 2013;19(5):432-41.
5. Cohen RA, Gullett JM, Porges EC, Woods AJ, Lamb DG, Bryant VE, et al. Heavy Alcohol Use and Age Effects on HIV-Associated Neurocognitive Function. Alcohol Clin Exp Res. 2019;43(1):147-57.
6. Ajasin D, Eugenin EA. HIV-1 Tat: Role in Bystander Toxicity. Front Cell Infect Mi. 2020;10:61.
7. Fulop T, Witkowski JM, Larbi A, Khalil A, Herbein G, Frost EH. Does HIV infection contribute to increased beta-amyloid synthesis and plaque formation leading to neurodegeneration and Alzheimer's disease? J Neurovirol. 2019;25(5):634-47.

8. Krogh KA, Wydeven N, Wickman K, Thayer SA. HIV-1 protein Tat produces biphasic changes in NMDA-evoked increases in intracellular Ca2+ concentration via activation of Src kinase and nitric oxide signaling pathways. J Neurochem. 2014;130(5):642-56.
9. Krogh KA, Lyddon E, Thayer SA. HIV-1 Tat activates a RhoA signaling pathway to reduce NMDA-evoked calcium responses in hippocampal neurons via an actin-dependent mechanism. J Neurochem. 2015;132(3):354-66.
10. Kirchhoff F. Analysis of Functional NMDA Receptors in Astrocytes. Methods Mol Biol. 2017;1677:241-51.
11. Chen L, Zhang H, Xu R, Li W, Zhao H, Yang Y, et al. Interaction of aquaporin 4 and N-methyl-D-aspartate NMDA receptor 1 in traumatic brain injury of rats. Iran J Basic Med Sci. 2018;21(11):1148-54.
12. Dadgostar E, Rahimi S, Nikmanzar S, Nazemi S, Naderi Taheri M, Alibolandi Z, et al. Aquaporin 4 in Traumatic Brain Injury: From Molecular Pathways to Therapeutic Target. Neurochem Res. 2022;47(4):860-71.
13. Dadgostar E, Tajiknia V, Shamsaki N, Naderi-Taheri M, Aschner M, Mirzaei H, et al. Aquaporin 4 and brain-related disorders: Insights into its apoptosis roles. Excli J. 2021;20:983-94.
14. Silva I, Silva J, Ferreira R, Trigo D. Glymphatic system, AQP4, and their implications in Alzheimer's disease. Neurol Res Pract. 2021;3(1):5.
15. St Hillaire C, Vargas D, Pardo CA, Gincel D, Mann J, Rothstein JD, et al. Aquaporin 4 is increased in association with human immunodeficiency virus dementia: implications for disease pathogenesis. J Neurovirol. 2005;11(6):535-43.
16. Xing HQ, Zhang Y, Izumo K, Arishima S, Kubota R, Ye X, et al. Decrease of aquaporin-4 and excitatory amino acid transporter-2 indicate astrocyte dysfunction for pathogenesis of cortical degeneration in HIV-associated neurocognitive disorders. Neuropathology. 2017;37(1):25-34.
17. Hu Q, Chen X. MiR-27a-3p Enhances Endometrial Cancer Growth and EMT by Targeting LIFR and Activating the p38/MAPK Pathways. Iran J Biotechnol. 2025;23(3):e4008.
18. Wei Z, Ding H, Li H, Yin D, Cao J. Eicosapentaenoic Acid Modulates TGF-β1/Smad3/ILK Pathway to Attenuate Renal Fibrosis: A Biotechnological Approach. Iran J Biotechnol. 2025;23(2):e4098.
19. Bandera A, Taramasso L, Bozzi G, Muscatello A, Robinson JA, Burdo TH, et al. HIV-Associated Neurocognitive Impairment in the Modern ART Era: Are We Close to Discovering Reliable Biomarkers in the Setting of Virological Suppression? Front Aging Neurosci. 2019;11:187.
20. Wang Y, Liu M, Lu Q, Farrell M, Lappin JM, Shi J, et al. Global prevalence and burden of HIV-associated neurocognitive disorder: A meta-analysis. Neurology. 2020;95(19):e2610-21.
21. Antinori A, Arendt G, Becker JT, Brew BJ, Byrd DA, Cherner M, et al. Updated research nosology for HIV-associated neurocognitive disorders. Neurology. 2007;69(18):1789-99.
22. Qi Y, Ailixire A, Gao Y, Li R, Li H. Current situation and prospect of HIV-associated neurocognitive disorder research in China: Epidemiology, research, diagnosis, and treatment status. Aids Rev. 2021;23(2):74-81.
23. Tice C, McDevitt J, Langford D. Astrocytes, HIV and the Glymphatic System: A Disease of Disrupted Waste Management? Front Cell Infect Mi. 2020;10:523379.
24. Dong H, Ye X, Zhong L, Xu J, Qiu J, Wang J, et al. Role of FOXO3 Activated by HIV-1 Tat in HIV-Associated Neurocognitive Disorder Neuronal Apoptosis. Front Neurosci-Switz. 2019;13:44.
25. Wu X, Dong H, Ye X, Zhong L, Cao T, Xu Q, et al. HIV-1 Tat increases BAG3 via NF-kappaB signaling to induce autophagy during HIV-associated neurocognitive disorder. Cell Cycle. 2018;17(13):1614-23.
26. Saiyed ZM, Gandhi N, Agudelo M, Napuri J, Samikkannu T, Reddy PVB, et al. HIV-1 Tat upregulates expression of histone deacetylase-2 (HDAC2) in human neurons: implication for HIV-associated neurocognitive disorder (HAND). Neurochem Int. 2011;58(6):656-64.
27. Paris JJ, Chen X, Anderson J, Qrareya AN, Mahdi F, Du F, et al. In vivo proton magnetic resonance spectroscopy detection of metabolite abnormalities in aged Tat-transgenic mouse brain. Geroscience. 2021;43(4):1851-62.
28. Agrawal L, Louboutin J, Reyes BAS, Van Bockstaele EJ, Strayer DS. HIV-1 Tat neurotoxicity: a model of acute and chronic exposure, and neuroprotection by gene delivery of antioxidant enzymes. Neurobiol Dis. 2012;45(2):657-70.
29. Hu G, Liao K, Yang L, Pendyala G, Kook Y, Fox HS, et al. Tat-Mediated Induction of miRs-34a & -138 Promotes Astrocytic Activation via Downregulation of SIRT1: Implications for Aging in HAND. J Neuroimmune Pharm. 2017;12(3):420-32.
30. Chauhan A, Turchan J, Pocernich C, Bruce-Keller A, Roth S, Butterfield DA, et al. Intracellular human immunodeficiency virus Tat expression in astrocytes promotes astrocyte survival but induces potent neurotoxicity at distant sites via axonal transport. J Biol Chem. 2003;278(15):13512-9.

31. Bachani M, Sacktor N, McArthur JC, Nath A, Rumbaugh J. Detection of anti-tat antibodies in CSF of individuals with HIV-associated neurocognitive disorders. J Neurovirol. 2013;19(1):82-8.
32. Li W, Li G, Steiner J, Nath A. Role of Tat protein in HIV neuropathogenesis. Neurotox Res. 2009;16(3):205-20.
33. Green MV, Thayer SA. NMDARs Adapt to Neurotoxic HIV Protein Tat Downstream of a GluN2A-Ubiquitin Ligase Signaling Pathway. J Neurosci. 2016;36(50):12640-9.
34. Skowronska K, Obara-Michlewska M, Czarnecka A, Dabrowska K, Zielinska M, Albrecht J. Persistent Overexposure to N-Methyl-D-Aspartate (NMDA) Calcium-Dependently Downregulates Glutamine Synthetase, Aquaporin 4, and Kir4.1 Channel in Mouse Cortical Astrocytes. Neurotox Res. 2019;35(1):271-80.
35. Zhao F, Deng J, Xu X, Cao F, Lu K, Li D, et al. Aquaporin-4 deletion ameliorates hypoglycemia-induced BBB permeability by inhibiting inflammatory responses. J Neuroinflamm. 2018;15(1):157.
36. Guo J, Mi X, Zhan R, Li M, Wei L, Sun J. Aquaporin 4 Silencing Aggravates Hydrocephalus Induced by Injection of Autologous Blood in Rats. Med Sci Monitor. 2018;24:4204-12.
37. Park H, Choi S, Kong M, Kang T. Dysfunction of 67-kDa Laminin Receptor Disrupts BBB Integrity via Impaired Dystrophin/AQP4 Complex and p38 MAPK/VEGF Activation Following Status Epilepticus. Front Cell Neurosci. 2019;13:236.
38. Cao J, Yao D, Li R, Guo X, Hao J, Xie M, et al. Digoxin Ameliorates Glymphatic Transport and Cognitive Impairment in a Mouse Model of Chronic Cerebral Hypoperfusion. Neurosci Bull. 2022;38(2):181-99.
39. Verheggen ICM, Van Boxtel MPJ, Verhey FRJ, Jansen JFA, Backes WH. Interaction between blood-brain barrier and glymphatic system in solute clearance. Neurosci Biobehav R. 2018;90:26-33.
40. Vandebroek A, Yasui M. Regulation of AQP4 in the Central Nervous System. Int J Mol Sci. 2020;21(5).
41. Naganawa S, Taoka T. The Glymphatic System: A Review of the Challenges in Visualizing its Structure and Function with MR Imaging. Magn Reson Med Sci. 2022;21(1):182-94.
42. Mostafavi H, Khaksarian M, Joghataei MT, Hassanzadeh G, Soleimani M, Eftekhari S, et al. Fluoxetin upregulates connexin 43 expression in astrocyte. Basic Clin Neurosci. 2014;5(1):74-9.
43. Chen S, Yang J, Kong F, Ren J, Hao K, Li M, et al. Overactivation of corticotropin-releasing factor receptor type 1 and aquaporin-4 by hypoxia induces cerebral edema. P Natl Acad Sci Usa. 2014;111(36):13199-204.
44. Zhu M, Lu C, Xia C, Qiao Z, Zhu D. Simvastatin pretreatment protects cerebrum from neuronal injury by decreasing the expressions of phosphor-CaMK II and AQP4 in ischemic stroke rats. J Mol Neurosci. 2014;54(4):591-601.
45. Cumbay MG, Watts VJ. Galphaq potentiation of adenylate cyclase type 9 activity through a Ca2+/calmodulin-dependent pathway. Biochem Pharmacol. 2005;69(8):1247-56.
46. Marcelo KL, Means AR, York B. The Ca(2+)/Calmodulin/CaMKK2 Axis: Nature's Metabolic CaMshaft. Trends Endocrin Met. 2016;27(10):706-18.
47. Huang H, Liao D, Liang L, Song L, Zhao W. Genistein inhibits rotavirus replication and upregulates AQP4 expression in rotavirus-infected Caco-2 cells. Arch Virol. 2015;160(6):1421-33.